Proteomic analysis of lithium-induced nephrogenic diabetes insipidus: Mechanisms for aquaporin 2 down-regulation and cellular proliferation

Jakob Nielsen*†, Jason D. Hoffert‡, Mark A. Knepper‡, Peter Agre§¶, Søren Nielsen*†, and Robert A. Fenton*†¶

*Water and Salt Research Center, University of Aarhus, DK-8000 Aarhus C, Denmark; †Institute of Anatomy, University of Aarhus, DK-8000 Aarhus C, Denmark; ‡Laboratory of Kidney and Electrolyte Metabolism, National Heart, Lung, and Blood Institute, National Institutes of Health, Bethesda, MD 20892; and §Department of Cell Biology, Duke University Medical Center, Durham, NC 27710

Contributed by Peter Agre, January 1, 2008 (sent for review December 11, 2007)

Lithium is a commonly prescribed mood-stabilizing drug. However, chronic treatment with lithium induces numerous kidney-related side effects, such as dramatically reduced aquaporin 2 (AQP2) abundance, altered renal function, and structural changes. As a model system, inner medullary collecting ducts (IMCD) isolated from rats treated with lithium for either 1 or 2 weeks were subjected to differential 2D gel electrophoresis combined with mass spectrometry and bioinformatics analysis to identify (*i*) signaling pathways affected by lithium and (*ii*) unique candidate proteins for AQP2 regulation. After 1 or 2 weeks of lithium treatment, we identified 6 and 74 proteins with altered abundance compared with controls, respectively. We randomly selected 17 proteins with altered abundance caused by lithium treatment for validation by immunoblotting. Bioinformatics analysis of the data indicated that proteins involved in cell death, apoptosis, cell proliferation, and morphology are highly affected by lithium. We demonstrate that members of several signaling pathways are activated by lithium treatment, including the PKB/Akt-kinase and the mitogen-activated protein kinases (MAPK), such as extracellular regulated kinase (ERK), c-Jun NH_2-terminal kinase (JNK), and p38. Lithium treatment increased the intracellular accumulation of β-catenin in association with increased levels of phosphorylated glycogen synthase kinase type 3β (GSK3β). This study provides a comprehensive analysis of the proteins affected by lithium treatment in the IMCD and, as such, provides clues to potential lithium targets in the brain.

differential gel electrophoresis (DIGE) | kidney | GSK3β | Akt kinase

Lithium administration is the most popular therapeutic approach to treat bipolar disorders, with 0.1% of the population receiving lithium (1, 2). In 50% of these patients, chronic lithium treatment is associated with altered renal function and nephrogenic diabetes insipidus (NDI) characterized by a defective urinary concentrating mechanism that manifests in polyuria, increased sodium excretion, and hypercholoremic metabolic acidosis (3). The polyuria is largely explained by decreased abundances of the vasopressin (AVP)-regulated aquaporin 2 and aquaporin 3 (AQP2 and AQP3) water channels in the collecting duct (4, 5). The renal sodium loss is likely to be caused by reduced expression of the epithelial sodium channel (ENaC) in the cortical and outer medullary collecting duct (6, 7). In addition, lithium induces increased expression of important acid-base transporting proteins including the H^+-ATPase and the anion exchanger type 1 (AE1) in the collecting duct (8). These changes may be, at least in part, attributable to an increase in the proportion of intercalated cells compared with principal cells (9), which is associated with increased cell proliferation and apoptosis of principal cells (10). Additionally, further "remodeling" of the kidney can occur with lithium treatment, including major structural changes such as medullary tubular cysts and tubular atrophy, resulting in tubulointerstitial fibrosis and renal failure (11).

Despite numerous studies documenting the consequences of chronic lithium treatment, little is known about the underlying mechanism and signaling pathways affected by lithium. In this study, we describe the use of differential gel electrophoresis (DIGE) combined with matrix-assisted laser desorption-ionization time-of-flight (MALDI-TOF) mass spectrometry (MS) and bioinformatics to identify proteins with altered abundance in the inner medullary collecting ducts (IMCD) of lithium-treated rats and their possible cellular function.

Results

Physiological Effect of Lithium Treatment. Chronic lithium administration resulted in a profound urinary concentrating defect. In both study 1 and study 2, water intake was significantly increased after 4 days of lithium treatment (Fig. 1*A*). During this time period, urine volumes changed correspondingly and were increased ≈3-fold after 1 week of lithium treatment and >6-fold after 2 weeks of lithium treatment [see Fig. 1*B* and supporting information (SI) Table 6]. Thus, the effects of lithium on renal water excretion were established at 1 week and progressed over the following week, indicating further changes in renal function. The observed polyuria was accompanied by a time-dependent reduction in AQP2 protein abundance in the IMCD (Fig. 1*C*), with AQP2 protein expression decreased to 58% of control rats at 1 week of lithium treatment and further decreased to 33% of control rats at 2 weeks of lithium treatment consistent with previous studies (10).

DIGE Combined with MALDI-TOF-TOF Identified Multiple Unique Proteins Regulated by Lithium. To identify proteins in the IMCD proteome with altered abundance in lithium-treated rats compared with control rats, we carried out 2D DIGE followed by tandem MS. On each of five 2D gels, the fluorescence of equivalent amounts of Cy3-labeled IMCD protein from lithium-treated rats and Cy5-labeled protein from control rats was detected with a laser-fluorescence scanner. A representative gel image is shown in Fig. 2. For statistical analysis, the fluorescence signals for each protein spot were normalized between gels, and protein spots with significantly changed signal intensities were chosen for identification (23‖ and 159 protein spots from weeks 1 and 2, respectively). Proteins were considered positively identified if (*i*) the total protein score (MS certainty estimate) based on the peptide fingerprint was ≥99% or (*ii*) the total protein score based on peptide fingerprint was ≥95% combined with a total ion score (tandem MS certainty

Author contributions: J.N. and R.A.F. designed research; J.N., J.D.H., and R.A.F. performed research; J.N., M.A.K., P.A., S.N., and R.A.F. analyzed data; and J.N., M.A.K., P.A., S.N., and R.A.F. wrote the paper.

The authors declare no conflict of interest.

¶To whom correspondence may be addressed. E-mail: rofe@ana.au.dk or pagre@cellbio.duke.edu.

This article contains supporting information online at www.pnas.org/cgi/content/full/0800001105/DC1.

‖In addition, 56 protein spots that did not have significantly different expression by DIGE analysis were chosen for identification.

www.pnas.org/cgi/doi/10.1073/pnas.0800001105

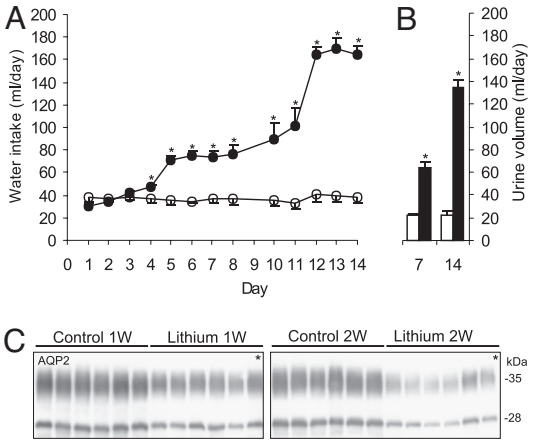

Fig. 1. Effects of lithium treatment on water balance and AQP2 protein expression in study 1. (*A*) Daily water intake was increased in the lithium-treated rats at day 4 and progressively increased until day 14. (*B*) Daily urine volume was increased in parallel with the water intake. (*C*) Immunoblotting of AQP2 in the IMCD showed decreased expression at 1 week and 2 weeks of lithium treatment compared with untreated control rats. *, $P < 0.05$.

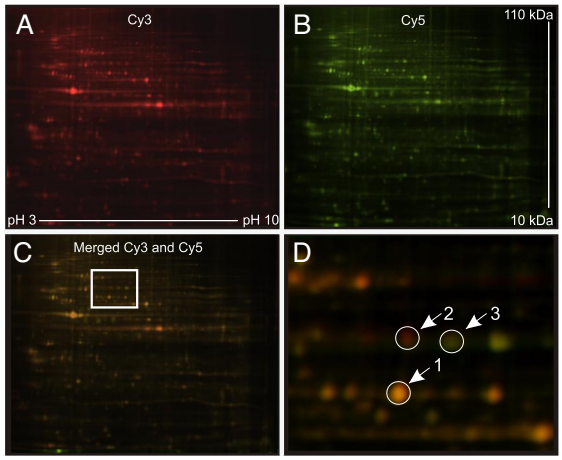

Fig. 2. Representative images of Cy3- and Cy5-labeled protein on a 2D gel. (*A*) Fluorescence of Cy3-labeled IMCD protein from lithium-treated rats shown as red pseudo-color. (*B*) Fluorescence of Cy5-labeled IMCD protein from control rats shown as green pseudo-color. (*C*) Merged image of *A* and *B* with box indicating magnified image in *D*. (*D*) Magnification of boxed section in *C*. Protein spots with equal protein abundance appear yellow (arrow 1), and proteins with increased or decreased protein expression in lithium-treated rats appear red (arrow 2) and green (arrow 3), respectively.

estimate) based on peptide sequence was ≥95%, and (*iii*) the molecular weight and the isoelectric point of the identified protein were consistent with the protein spot location on the 2D gel. These parameters resulted in identification of 6 and 74 different proteins with changed expression at 1 and 2 weeks, respectively (Tables 1 and 2).

An additional animal study, with physiological parameters observed similar to study 1 (SI Table 6), was performed followed by immunoblotting to confirm the abundance changes in several of the proteins identified by using MALDI-TOF-TOF (Fig. 3 and SI Table 7). The changes in protein abundance observed by immunoblotting showed a general correlation with the changes in protein spot intensities obtained by using DIGE (Fig. 4).

Pathway Analysis Identified Cell Death and Apoptosis as Major Cellular Functions Affected by Lithium. To explore the functional roles of the changed proteins in lithium-treated rats and to generate hypothesis for further studies, we performed bioinformatic pathway analysis using Ingenuity Pathway Analysis (IPA) software. Because we were interested in identifying candidate proteins and signaling mechanisms involved in the total cellular response to lithium, both 1- and 2-week time points were included in the pathways analysis. The IPA analysis revealed that a large fraction of the proteins we identified were associated with cell structure (e.g., annexin 2, annexin 5, ezrin, lamin A), cell death (e.g., adenine phosphoribosyltransferase, mortalin, cyclophilin A), and apoptosis (e.g., peroxiredoxin-5, programmed cell death protein 6, retinaldehyde dehydrogenase 3) (Table 3, SI Table 8). In addition, based on the IPA analysis, we proposed that signaling pathways involving the PKB/Akt-kinase and the mitogen-activated protein kinases (MAPK)—including extracellular regulated kinase (ERK), c-Jun NH_2-terminal kinase (JNK), and p38 MAPK—could be involved in mediating both the lithium-induced changes on cell viability and cell structure as well as the reduced expression of AQP2 observed during chronic lithium treatment.

Lithium Treatment Increases Phosphorylation of PKB (Akt) and Glycogen Synthase Kinase Type 3β (GSK3β). To assess these predictions, changes in both protein abundance and phosphorylation state of these kinases were analyzed (Fig. 5, Table 4 , and SI Table 9). Total protein abundance of Akt was unchanged at both 1 and 2 weeks of lithium treatment compared with control rats, whereas the phosphorylated forms pS473Akt and pT308Akt were increased >2-fold.

After 1 week of lithium treatment, the downstream cell-cycle controlling protein P27/Kip1 also was decreased, possibly because of degradation via a phospho-Akt-mediated mechanism. In the same pathway, phosphorylated (active) Akt further phosphorylates GSK3β at serine 9 thereby inhibiting GSK3β kinase activity. Consistent with this pathway, the abundance of phosphorylated pS9-GSK3β was increased 2.5-fold and 4-fold at 1 and 2 weeks of lithium treatment, respectively.

Table 1. Proteins identified by MALDI-TOF-TOF after 1 week of lithium treatment

Protein name	Lithium/Control	
78-kDa glucose-regulated protein (GRP78)	1.6	
Cathepsin D	1.6	↑
Fatty acid-binding protein	0.65*	
Myosin light polypeptide 6	0.57	
Prohibitin	1.5*	↑
T-plastin (Plastin-3)	1.8	↕
Annexin 5	0.98 NS	↕
Carbonic anhydrase 2	1.1 NS	↑
Elongation factor Tu (eEF1A-1)	1.7 NS	↑
Glutathione *S*-transferase μ 1	0.79 NS	↑
Glutathione *S*-transferase π	1.07 NS	↑
Heat shock 70-kDa protein 1B	0.90 NS	↕
Heat shock 70-kDa protein 1-like	0.90 NS	↓
Hypoxanthine-guanine phosphoribosyltransferase	1.4 NS	↑
NADH dehydrogenase	0.64 NS	↑
Protein disulfide-isomerase A3 (ERp60)	1.1/1.4 NS	↑
Retinaldehyde dehydrogenase 3	1.3 NS	↓
Superoxide dismutase [Cu-Zn]	0.85/1.2 NS	↑
Thioredoxin domain-containing protein 4	1.1 NS	↑
Transketolase	1.2 NS	↑
β-Actin	1.1* NS	↑

Names of identified proteins and the ratio of protein abundance (lithium/control) after 1 week of lithium treatment. Additional identified proteins with nonsignificant change (NS) at 1 week but significant changes at 2 weeks of lithium treatment are included in the table. The arrows indicate the change in protein abundance observed after 2 weeks of lithium treatment. Bidirectional arrows indicate that both up- and down-regulation were observed in different spots. Unmarked values were identified by MS with certainty scores >99%. Values marked with asterisks (*) were identified with certainty score >95% by both MS and tandem MS.

PHYSIOLOGY

Table 2. Proteins identified by MALDI-TOF-TOF after 2 weeks of lithium treatment

Protein name	Lithium/Control
14-3-3ε and 14-3-3θ	3.2 and 0.44
26S proteasome non-ATPase regulatory subunits 8 and 13	2.7 and 1.5
3-Hydroxyacyl-CoA dehydrogenase type 2	2.9*
Aconitase	1.7
Actin-like protein 3	1.9
Adenine phosphoribosyltransferase	3.1/2.2
Adenosine kinase	2.1
Aldose 1-epimerase	0.52
Aldose reducatse	0.51*
Annexin 2 and 4 and 5	0.64 and 1.5 and 1.7*
ATP synthase β and δ chain	1.7* and 2.5
Calcyclin	0.61
Calmodulin	0.62*
Carbonic anhydrase 2	2.0*
Cathepsin D	3.4
Cofilin-1	1.6
Creatine kinase B type	2.4
Cyclophilin A	1.6/1.8/2.4
Cytochrome *c* oxidase subunits 5A and 5B	1.6* and 2.3*
Dynein light chain 2A	4.3*
ECH1 (Q62651)	1.6
Electron transfer flavoprotein β-subunit	2.7
Elongation factor Tu (eEF1A-1)	1.8
Eukaryotic translation initiation factor 3 subunit 12	5.8
Ezrin	2.2
Ferritin light chain 1	2.5
Fructose-bisphosphate aldolase A	1.5/0.64*
Glutathione *S*-transferase μ1 and π	2.9 and 3
GTP-binding nuclear protein Ran	1.7*
Heat shock 27-kDa protein	0.5*
Heat shock 70-kDa protein 1B	0.64/1.7
Heat shock 70-kDa protein 1-like	0.64*
Hypoxanthine-guanine phosphoribosyltransferase	1.7
Lamin A	1.6/5.5
L-lactate dehydrogenase A chain	0.45/2.3
Malate dehydrogenase	0.47/1.8
Mortalin	2.4*
NADH dehydrogenase	1.9/2.2
Nerve growth factor-induced protein 42A	0.51*
Neurostimulating peptide (HCNP)	1.9/2.4
NSFL1 cofactor p47	1.5/1.9
Nucleoside diphosphate kinase B	1.6*
Oxalosuccinate decarboxylase	0.6
Peroxiredoxin-5	1.8*
Phosphoglycerate mutase isozyme B	1.7/2.7
Programmed cell death protein 6	2.1
Prohibitin	2.7*
Proteasome activator complex subunit 2	1.8/2.7/3.2*
Proteasome subunit β types 1 and 9	4.7 and 2.6*
Protein disulfide-isomerase A3 (ERp60)	2.0*
Retinaldehyde dehydrogenase 3	0.62
SNAP-25-interacting protein	1.8
Stress-induced-phosphoprotein 1 (STI1)	1.6
Superoxide dismutase [Cu-Zn]	1.8
Thioredoxin domain-containing protein 4	1.6
T-plastin (Plastin-3)	0.64/1.7
Transketolase	1.8
Triosephosphate isomerase	1.8
Tropomyosin-1 α chain	0.44
Tumor rejection antigen gp96	1.5
Ubiquinol-cytochrome *c* reductase iron-sulfur subunit	1.8*
Uridine monophosphate kinase	2.7
Vacuolar protein sorting-associated protein 29	1.6*
α-Crystallin B chain	0.62*
α-Glucosidase 2	2.3
β-Actin	1.7*

Identified proteins and the ratio of protein abundance (lithium/control) after 2 weeks of lithium treatment. Unmarked values were identified by MS with certainty scores >99%. Values marked with asterisks (*) were identified with certainty score >95% by both MS and tandem MS. Multiple numbers are the same protein identified in different spots.

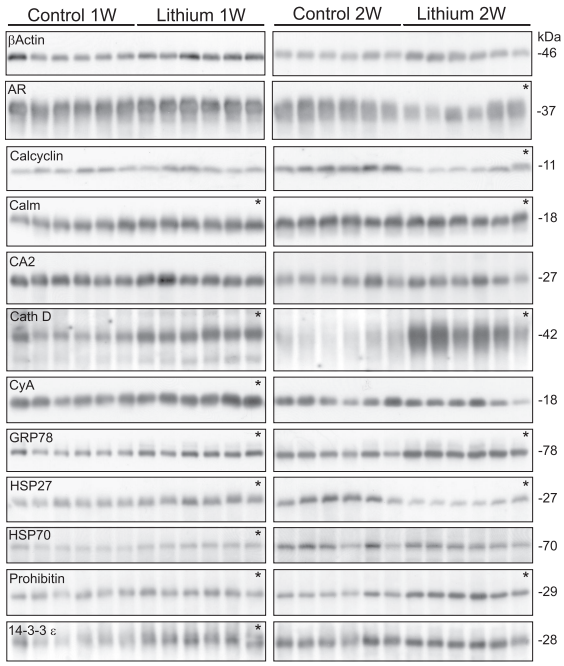

Fig. 3. Confirmatory immunoblotting for IMCD proteins identified as changed by lithium treatment. Each row shows a representative immunoblot, and each lane is loaded with a sample from a different rat (n = 6 rats per treatment). *, $P < 0.05$.

Lithium Treatment Increases Phosphorylation of ERK, JNK, and P38. ERK, JNK, and P38 MAPK also were affected by lithium. Although phosphorylated pERK2 was increased only at 2 weeks, total ERK2 abundance was increased at both 1 and 2 weeks (Fig. 5, Table 4). Total JNK1 and JNK2 abundance as well as (active) phosphorylated pJNK1 were increased at both time points, alongside total and phosphorylated P38 (activated) (Fig. 5, Table 4). One target of P38 MAPK is phosphorylation of HSP27 (identified with DIGE-MALDI-TOF-TOF). HSP27, which is important for cell survival during cell stress (12), was increased at 1 week of lithium treatment but markedly decreased after 2 weeks of lithium treatment (Fig. 3, Table 2).

Lithium Treatment Results in Increased β-Catenin and E-Cadherin Abundance. A potential target for GSK3β is β-catenin, which is phosphorylated by GSK3β, resulting in its proteasomal degradation

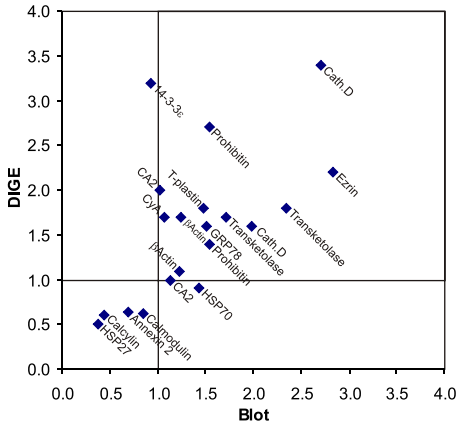

Fig. 4. Correlation of changes in protein expression determined by DIGE analysis versus immunoblotting. The ratio of protein expression in lithium/control as determined by immunoblotting and DIGE analysis are expressed on the *x* axis and *y* axis, respectively. Proteins identified at both 1 and 2 weeks are included.

Table 3. Summary of IPA analysis

Cellular function	Number of proteins
Cell death (apoptosis)	29 (22)
Cell growth and proliferation	22
Cell morphology	10
Nucleic Acid Metabolism	9
Small molecule biochemistry	23
Cell signaling	40
Carbohydrate metabolism	23

Shown are the number of identified proteins associated with molecular pathways and cellular function as determined by IPA and ordered by decreasing IPA analysis significance score.

(13). Thus, a decrease in active pS9-GSK3β would be predicted to result in increased β-catenin. Indeed, after 2 weeks of lithium treatment, β-catenin abundance is increased significantly (Fig. 5, Table 4) compared with controls. Increased β-catenin not associated with the cell-to-cell cadherin complex can accumulate intracellularly affecting the Wnt-signaling cascade. To examine this possibility, immunolabeling of β-catenin in control or lithium-treated rats was performed (Fig. 6). In both control rats and rats after 1 week of lithium treatment, β-catenin labeling is localized predominantly to the basolateral plasma membrane domain. In contrast, in rats after 2 weeks of lithium treatment, there is a marked increase in intracellular β-catenin labeling, suggesting accumulation of β-catenin within the principal cell. Because β-catenin is a central component of the cadherin cell-adhesion complex, the redistribution of β-catenin may affect other proteins involved in cell-to-cell adhesion. Indeed, the abundance of E-cadherin was increased after lithium treatment (Fig. 5, Table 4), although this change was not associated with altered cellular distribution (data not shown).

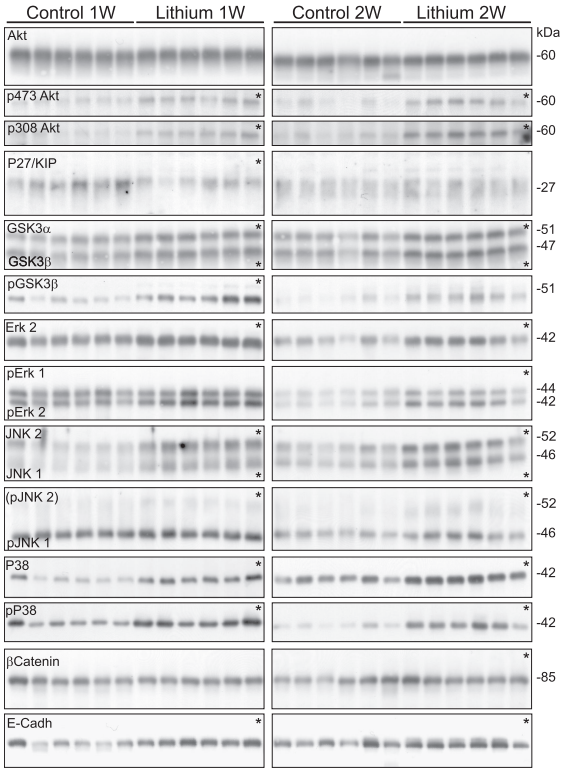

Fig. 5. Immunoblotting for proteins predicted by pathway analysis to be involved in lithium-induced changes. Each row shows a representative immunoblot, and each lane is loaded with a sample from a different rat ($n = 6$ rats per treatment). *, $P < 0.05$.

Table 4. Summary of immunoblots of proteins predicted by pathway analysis (IPA) to be affected by lithium

	Length of lithium treatment	
Protein name	1 week	2 week
Akt	109 ± 4	110 ± 7
p473Akt	253 ± 16*	270 ± 25*
p308Akt	231 ± 30*	260 ± 7*
P27/KIP	58 ± 8*	117 ± 9
GSK3α	132 ± 5*	131 ± 4*
GSK3β	136 ± 4*	132 ± 4*
pGSK3β	258 ± 10*	416 ± 48*
Erk 2	133 ± 2*	169 ± 17*
Erk 1/2	120 ± 10	142 ± 13*
JNK1	295 ± 20*	182 ± 16*
JNK2	231 ± 14*	179 ± 15*
pJNK1	122 ± 6*	149 ± 9*
P38	268 ± 27*	197 ± 17*
pP38	200 ± 10*	426 ± 46*
β-Catenin	106 ± 2	144 ± 2*
E-cadherin	183 ± 10*	142 ± 9*

Controls were normalized to 100. *, $P < 0.05$ versus control at 1 week and control at 2 weeks, respectively. Phosphorylated proteins are labeled with the prefix "p."

Discussion

The present study uses a proteomics approach, coupled with pathways analysis, to identify unique proteins that are involved in the pathogenesis of lithium-induced NDI. Moreover, we examined the activation state of a number of key cellular signaling pathways to further investigate the cellular changes induced by lithium.

The well established lithium protocol used in our study resulted in development of a severe polyuria within 7 days that progressed in magnitude throughout the duration of the study. For the pro-

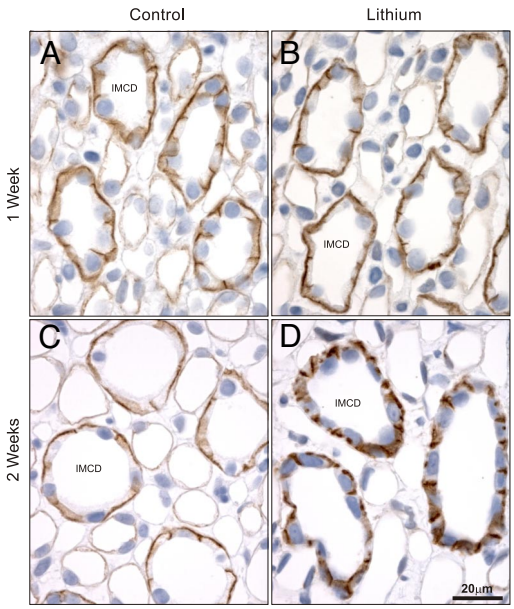

Fig. 6. Immunoperoxidase labeling of β-catenin in the inner medulla. In control rats (*A* and *C*), β-catenin labeling is localized predominantly to the basolateral plasma membrane domain. After 1 week of lithium (*B*), labeling is unchanged compared with control rats, but after 2 weeks (*D*), there is a marked increase in intracellular β-catenin labeling within the principal cell. (Scale bar: 20 μm.)

teomic analysis, the two time points examined were specifically chosen as: (*i*) after 7 days of lithium treatment, the proteins with altered abundance may be involved in the mechanism that results in down-regulation of AQP2 and the subsequent onset of polyuria; and (*ii*) after 14 days of lithium treatment, proteins identified may be important for the lithium-induced structural changes in the kidney that occur with prolonged lithium treatment. However, it is important to emphasize that the cellular responses to lithium treatment identified from this study could be direct responses (e.g., responses to increased phosphorylation of transcription factors by "lithium-regulated kinases") or indirect responses that are not an immediate consequence of lithium-mediated signaling (e.g., changes in protein abundance attributable to the reduced interstitial osmolality that occurs from prolonged polydipsia and polyuria). The indirect effects of lithium are likely to be diverse and may include several categories of responses, such as (*i*) induction of transcription factors downstream of transcription factors immediately activated by lithium; (*ii*) secondary changes in circulating hormone levels (such as AVP); or (*iii*) responses to increased tubular flow occurring in polyuria. This study does not attempt to discriminate between these different types of responses. Furthermore, several of the proteins identified in this study are key regulators in more than one intracellular signaling process; thus, the relative effect of lithium on each individual pathway can only be postulated.

Proteomic analysis using stringent parameters to avoid false-positive identifications resulted in identification of 6 and 74 different proteins with altered abundance at 1 and 2 weeks, respectively. Although a direct correlation was observed between the changes in abundance from confirmatory immunoblotting and the changes in protein spot intensities obtained by using DIGE analysis, the magnitude of the changes between the two techniques differed substantially (Fig. 4). This difference may be explained, in part, by the possibility that posttranslational modifications result in proteins migrating to several different spots on the 2D gel. For example, after 2 weeks of lithium treatment, HSP70 was identified in two different protein spots with decreased and increased protein expression, whereas the total protein expression was unchanged by immunoblotting, suggesting a shift between two posttranslational states of HSP70 rather than a change in total abundance. Moreover, if only one of multiple spots of a shifted protein is identified on the DIGE gel, the protein expression (based on DIGE) may appear changed while the total protein abundance is unchanged based on immunoblotting (e.g., CA2 or 14-3-3ε). Thus, the list of proteins identified by DIGE and MALDI-TOF-TOF represents a list of proteins with changed expression in a specific posttranslational state. Below, we discuss some of the major regulatory targets identified and propose their role in lithium-induced NDI.

Regulation of PKB/Akt by Lithium and Its Role in Cell Survival. The active forms of Akt, pS473Akt and pT308Akt, were increased >2-fold after both 1 and 2 weeks of lithium treatment. Akt/PKB acts as a critical junction in cell signaling within all cells of higher eukaryotes. One of the key actions of Akt is to block apoptosis by blocking the function of proapoptotic proteins (such as Bcl-2), and promoting cell survival through activation of NF-κB signaling (14). Chronic lithium treatment causes a multitude of structural changes within the kidney. For example, despite increased proliferation of principal cells, the proportion of intercalated cells to principal cells increases after 4 weeks of lithium treatment, suggesting that there is a decrease in principal cell viability (9, 10). The observed increase in Akt activation could be a survival response by the principal cell to limit apoptosis and the trigger for induced cell proliferation. In support of this finding, lithium treatment decreases the abundance of the p27/Kip1 cyclin-dependent kinase inhibitor, thus limiting p27 localization to the nucleus and attenuating its cell-cycle inhibitory effects. The increased abundance of 14-3-3ε, which binds to p27 and sequesters it in the cytoplasm, and of HSP27, which causes degradation of p27, adds further credence to this pathway.

Increased HSP27, which binds to Akt, is a common response to cell stress, leading to cytoskeleton reorganization (12). This reorganization of the principal cell cytoskeleton possibly could play a direct role in the diminished AQP2 trafficking apparent after lithium treatment (15). Additionally, Akt-dependent phosphorylation and inhibition of GSK3 (see below) is proposed to drive cell proliferation by limiting the GSK3-mediated proteasomal degradation of proteins involved in cell-cycle entry, such as G_1 cyclins and the transcription factors c-*jun* and c-*myc*. Together, our results suggest that Akt signaling pathways are likely responsible for the marked principal cell proliferation observed with lithium treatment.

Phosphorylation of GSK3β. GSK3, which is inhibited noncompetitively by lithium (16, 17), has been studied extensively for its role in cell proliferation and epithelial-mesenchymal transition (13). In our study, lithium treatment resulted in a marked increase in phosphorylated (inactive) GSK3β, in line with previous studies (18). Because GSK3β is a target for phosphorylation by Akt, the increased *p*-Akt observed with lithium treatment is the potential upstream regulator of this signaling cascade (see above). In one of its many cellular functions, GSK3β functions as a negative regulator of the Wnt/beta-catenin (β-catenin) pathway by phosphorylating β-catenin (see below). Overexpression of GSK3 has been shown to make cells more sensitive to proapoptotic stimuli (19); thus, a decrease in its activity also may enhance cell survival.

A direct role of GSK3β in lithium-induced down-regulation of AQP2 abundance has not been demonstrated. However, it has been shown that inhibition of GSK3β by lithium results in enhanced renal COX2 expression in interstitial cells, leading to an increase in local PGE(2) excretion (18), that in turn may counteract AVP actions by causing endocytic retrieval of AQP2 from the collecting duct plasma membrane, thus impairing urinary concentrating ability (20). GSK3β knockout mice die from liver degeneration (21); thus, the consequence of GSK3β gene deletion on kidney function has yet to be examined. (A recent report has demonstrated that a collecting duct-specific gene knockout of GSK3β results in an impaired maximal urinary concentrating ability and a reduced increase in AQP2 mRNA levels after water restriction.**)

Increased Intracellular Accumulation of β-Catenin. β-Catenin not only regulates cell-to-cell adhesion as a protein interacting with cadherin but also functions as a component of the Wnt signaling pathway. When not assembled in complexes with cadherins, β-catenin forms an intracellular complex with axin that is phosphorylated by GSK3β, creating a signal for the rapid ubiquitin-dependent degradation of β-catenin by proteosomes. However, if GSK3β is inactivated, as we observed during lithium treatment, β-catenin can accumulate intracellularly and subsequently translocate to the nucleus where it serves as an activator of T cell factor (Tcf)-dependent transcription, leading to an increased expression of several specific target genes (22). After 2 weeks of lithium treatment, we showed a large increase in the intracellular abundance of β-catenin within the IMCD. Thus, it is plausible that lithium treatment further results in translocation of β-catenin to the IMCD cell nucleus, where it can regulate transcription of target genes. A previous study has reported that the effect of lithium on AQP2 down-regulation is mediated by a transcriptional mechanism (23). Interestingly, using bioinformatics we discovered that both the mouse and rat AQP2 gene 5′ flanking regions contain several

**Rao R, Hao C, Golovin A, Patel S, Woodgett J, Harris R, Breyer M, Collecting Duct Selective Gene Knockout of Glycogen Synthase Kinase 3β Impairs the Renal Response to Vasopressin. Renal Week 2007, October 31–November 5, 2007, San Francisco, CA, abstr. SA-FC142.

consensus sites for TCF, thus AQP2 gene transcription may be regulated directly by TCF-dependent transcription. Alternatively, TCF may regulate the abundance of other hierarchical transcription factors that subsequently modulate AQP2 expression. Furthermore, TCF-dependent transcription has been demonstrated to regulate a number of proteins involved in cell-cycle entry; thus, it also may play a role in the principal cell proliferation observed with lithium treatment. Direct analysis of these hypothesis using cell-based systems will form the basis of future work.

Other Kinase-Mediated Signaling Cascades. Lithium treatment resulted in either increased abundance or increased phosphorylation of JNK, P38, and MAPK/ERK. Increased *p*-Akt, via the apoptosis signal-regulating kinase 1 (ASK1), is a potential mediator of both JNK and P38 signaling pathways. Both JNK and P38 function in independent protein kinase cascades transducing cellular stress signals. Additionally, P38 is centrally involved in apoptosis and cytoskeleton reorganization after cell stress via its interaction with HSP27 (see above).

ERK is a classical MAPK that is ubiquitously expressed and can be activated by numerous stimuli such as growth factors. Stimulation of the ERK signaling cascade modulates numerous cellular functions, including cellular proliferation, differentiation, and survival. Interestingly, ERK inhibitors have been shown to block AVP-induced increases in AQP2 expression (24). Thus, increased ERK activation after lithium treatment may be a cellular response to limit down-regulation of AQP2.

Conclusion

Using a stringent proteomics approach, we have identified 77 different proteins within the IMCD that are affected, either directly or indirectly, by lithium treatment. The proteins identified have a variety of functions, including signal transduction, regulation of gene expression, cytoskeletal organization, cellular reorganization, apoptosis, and cell proliferation. A number of these proteins are ubiquitously expressed, such as GSK3β, and as such also may be involved in the actions of lithium within the brain. Our studies clearly demonstrate that the cellular effects of lithium treatment are broad and complex, and as such a single pathway leading to reduced AQP2 expression and subsequent polyuria is unlikely. However, our current study has identified numerous unique proteins that may play a role in AQP2 regulation and thus opens up numerous avenues of future research.

Concise Methods

Animal Protocol for Proteomics Study (Study 1) and Confirmatory Blotting (Study 2). All animal protocols were approved by the boards of the Institute of Anatomy and Institute of Clinical Medicine, University of Aarhus, according to the licenses for the use of experimental animals issued by the Danish Ministry of Justice. Male Wistar rats were housed individually in normal cages. Rats were given daily food rations consisting of (per 200 g of body weight) 20 g of rat chow supplemented with 1.7 mmol of NaCl (total Na intake was 3.4 mmol/200 g of body weight) and 20 ml of tap water. Lithium-treated rats received 0.8 mmol of LiCl per 200 g of body weight. All rats had free access to water. In study 1, the number of animals were: control, $n = 10$; lithium-treated, $n = 22$. In study 2, the number of animals were: control, $n = 12$ and lithium-treated, $n = 20$. Half of the rats in each study were treated for 1 week, and the other half were treated for 2 weeks. The two lithium-treated rats with the highest urine output and the two lithium-treated rats with the lowest urine output at the end of the study periods were excluded from analysis. Urine was collected over 24-h periods. After 7 and 14 days of treatment, rats were anesthetized with isoflurane, blood was collected from the inferior vena cava, kidneys were rapidly removed, the inner medulla was dissected, and IMCD tubules were prepared.

IMCD Tubule Preparation. The protocol for IMCD tubule suspension preparation has been described in ref. 25.

DIGE Analysis and Protein Identification. DIGE was performed as described in ref. 26.

Semiquantitative Immunoblotting, Immunohistochemistry, and Antibodies. After preparation of total protein from IMCD tubules, semiquantitative immunoblotting was performed as described in ref. 6. Results are listed as the relative band densities between the groups. The immunohistochemistry technique was described extensively in ref. 6. A minimum of four control or four lithium-treated rat kidneys were examined, and representative data are shown. Light microscopy was carried out with a Leica DMRE microscope (Leica Microsystems). For the list of antibodies used for immunoblotting and immunohistochemistry, including information about host animal, company, and catalogue number, see SI Table 10.

Presentation of Data and Statistical Analyses. Quantitative data are presented as mean ± SE. Data were analyzed by one-way ANOVA followed by Bonferroni's multiple-comparisons test. Multiple-comparisons tests were applied only when a significant difference was determined in the ANOVA ($P < 0.05$). *P* values <0.05 were considered statistically significant.

ACKNOWLEDGMENTS. We thank Angel Aponte at the Proteomics Core facility at the National Heart, Lung, and Blood Institute for expert assistance. The Water and Salt Research Center at the University of Aarhus is established and supported by the Danish National Research Foundation (Danmarks Grundforskningsfond). J.N. was supported by the foundation of A. P. Møller og Hustru Chastine McKinney Møllers Fond til almene Formal-Fonden til Lægevidenskabens Fremme. R.A.F. is supported by a Marie Curie Intra-European Fellowship and the Danish National Research Foundation. Funding to M.A.K. was provided by the Intramural Budget of the National Heart, Lung, and Blood Institute (National Institutes of Health Project Z01-HL001285). Further support for this study was provided by Marie Curie Research Training Networks (RTN) program ''AQUA(GLYCERO)PORINS.''

1. Freeman MP, Freeman SA (2006) Lithium: Clinical considerations in internal medicine. *Am J Med* 119:478–481.
2. Peet M, Pratt JP (1993) Lithium: Current status in psychiatric disorders. *Drugs* 46:7–17.
3. Timmer RT, Sands JM (1999) Lithium intoxication. *J Am Soc Nephrol* 10:666–674.
4. Kwon T-H, *et al*. (2000) Altered expression of renal AQPs and Na(+) transporters in rats with lithium-induced NDI. *Am J Physiol* 279:F552–F564.
5. Marples D, Christensen S, Christensen EI, Ottosen PD, Nielsen S (1995) Lithium-induced downregulation of aquaporin 2 water channel expression in rat kidney medulla. *J Clin Invest* 95:1838–1845.
6. Nielsen J, *et al*. (2003) Segment-specific ENaC downregulation in kidney of rats with lithium-induced NDI. *Am J Physiol* 285:F1198–F1209.
7. Thomsen K, Bak M, Shirley DG (1999) Chronic lithium treatment inhibits amiloride-sensitive sodium transport in the rat distal nephron. *J Pharmacol Exp Ther* 289:443–447.
8. Kim Y.-H., *et al*. (2003) Altered expression of renal acid-base transporters in rats with lithium-induced NDI. *Am J Physiol* 285:F1244–F1257.
9. Christensen BM, *et al*. (2004) Changes in cellular composition of kidney collecting duct cells in rats with lithium-induced. NDI *Am J Physiol* 286:C952–C964.
10. Christensen BM, Kim Y-H, Kwon T-H, Nielsen S (2006) Lithium treatment induces a marked proliferation of primarily principal cells in rat kidney inner medullary collecting duct. *Am J Physiol* 291:F39–F48.
11. Markowitz GS, *et al*. (2000) Lithium nephrotoxicity: A progressive combined glomerular and tubulointerstitial nephropathy. *J Am Soc Nephrol* 11:1439–1448.
12. Garrido C, *et al*. (2006) Heat shock proteins 27 and 70: Anti-apoptotic proteins with tumorigenic properties. *Cell Cycle* 5:2592–2601.
13. Doble BW, Woodgett JR (2007) Role of glycogen synthase kinase-3 in cell fate and epithelial-mesenchymal transitions. *Cells Tissues Organs* 185:73–84.
14. Manning BD, Cantley LC (2007) AKT/PKB signaling: Navigating downstream. *Cell* 129:1261–1274.
15. Nielsen S (2002) Aquaporins in the kidney: From molecules to medicine. *Physiol Rev* 82:205–244.
16. Stambolic V, Ruel L, Woodgett JR (1996) Lithium inhibits glycogen synthase kinase-3 activity and mimics wingless signalling in intact cells. *Curr Biol* 6:1664–1668.
17. Klein PS, Melton DA (1996) A molecular mechanism for the effect of lithium on development. *Proc Natl Acad Sci USA* 93:8455–8459.
18. Rao R, *et al*. (2005) Lithium treatment inhibits renal GSK-3 activity and promotes cyclooxygenase 2-dependent polyuria. *Am J Physiol* 288:F642–F649.
19. Bijur GN, De SP, Jope RS (2000) Glycogen synthase kinase-3β facilitates staurosporine- and heat shock-induced apoptosis: Protection by lithium. *J Biol Chem* 275:7583–7590.
20. Zelenina M, *et al*. (2000) Prostaglandin E(2) interaction with AVP: Effects on AQP2 phosphorylation and distribution. *Am J Physiol* 278:F388–F394.
21. Hoeflich KP, *et al*. (2000) Requirement for glycogen synthase kinase-3β in cell survival and NF-κB activation. *Nature* 406:86–90.
22. Novak A, Dedhar S (1999) Signaling through β-catenin and Lef/Tcf. *Cell Mol Life Sci* 56:523–537.
23. Li Y, Shaw S, Kamsteeg EJ, Vandewalle A, Deen PM (2006) Development of lithium-induced nephrogenic diabetes insipidus is dissociated from adenylyl cyclase activity. *J Am Soc Nephrol* 17:1063–1072.
24. Umenishi F, Narikiyo T, Vandewalle A, Schrier RW (2006) cAMP regulates vasopressin-induced AQP2 expression via protein kinase A-independent pathway. *Biochim Biophys Acta* 1758:1100–1105.
25. Chou CL, DiGiovanni SR, Luther A, Lolait SJ, Knepper MA (1995) Oxytocin as an antidiuretic hormone II: Role of V2 vasopressin receptor. *Am J Physiol* 269:F78–F85.
26. Hoffert JD, van Balkom BW, Chou CL, Knepper MA (2004) Application of difference gel electrophoresis to the identification of inner medullary collecting duct proteins. *Am J Physiol* 286:F170–F179.